



HAL
open science

Anomalous energy exchanges and Wigner function negativities in a single qubit gate

Maria Maffei, Cyril Elouard, Bruno Goes, Benjamin Huard, Andrew Jordan,
Alexia Auffèves

► **To cite this version:**

Maria Maffei, Cyril Elouard, Bruno Goes, Benjamin Huard, Andrew Jordan, et al.. Anomalous energy exchanges and Wigner function negativities in a single qubit gate. *Physical Review A*, 2023, 107 (2), pp.023710. 10.1103/PhysRevA.107.023710 . hal-03833031





HAL Id: hal-03833031

<https://hal.science/hal-03833031>

Submitted on 25 Aug 2023

HAL is a multi-disciplinary open access archive for the deposit and dissemination of scientific research documents, whether they are published or not. The documents may come from teaching and research institutions in France or abroad, or from public or private research centers.

L'archive ouverte pluridisciplinaire **HAL**, est destinée au dépôt et à la diffusion de documents scientifiques de niveau recherche, publiés ou non, émanant des établissements d'enseignement et de recherche français ou étrangers, des laboratoires publics ou privés.

Anomalous energy exchanges and Wigner-function negativities in a single-qubit gateMaria Maffei ¹, Cyril Elouard ², Bruno O. Goes ¹, Benjamin Huard,³ Andrew N. Jordan,^{4,5} and Alexia Auffèves ^{1,6}¹*Université Grenoble Alpes, CNRS, Grenoble INP, Institut Néel, 38000 Grenoble, France*²*Inria, ENS Lyon, LIP, F-69342, Lyon Cedex 07, France*³*Ecole Normale Supérieure de Lyon, CNRS, Laboratoire de Physique, F-69342 Lyon, France*⁴*Institute for Quantum Studies, Chapman University, 1 University Drive, Orange, California 92866, USA*⁵*Department of Physics and Astronomy, University of Rochester, Rochester, New York 14627, USA*⁶*MajuLab, International Joint Research Unit UMI 3654, CNRS, Université Côte d'Azur, Sorbonne Université, National University of Singapore, Nanyang Technological University, Singapore*

(Received 26 October 2022; accepted 30 January 2023; published 13 February 2023)

Anomalous weak values and the Wigner function's negativity are well-known witnesses of quantum contextuality. We show that these effects occur when analyzing the energetics of a single-qubit gate generated by a resonant coherent field traveling in a waveguide. The buildup of correlations between the qubit and the field is responsible for bounds on the gate fidelity, but also for a nontrivial energy balance recently observed in a superconducting setup. In the experimental scheme, the field is continuously monitored through heterodyne detection and then postselected over the outcomes of a final qubit's measurement. The postselected data can be interpreted as the field's weak values and can show anomalous values in the variation of the field's energy. We model the joint system dynamics with a collision model, gaining access to the qubit-field entangled state at any time. We find an analytical expression of the quasiprobability distribution of the postselected heterodyne signal, i.e., the conditional Husimi-Q function. The latter grants access to all the field's weak values: we use it to obtain that of the field's energy change and display its anomalous behavior. Finally, we derive the field's conditional Wigner function and show that anomalous weak values and Wigner function negativities arise for the same values of the gate's angle.

DOI: [10.1103/PhysRevA.107.023710](https://doi.org/10.1103/PhysRevA.107.023710)**I. INTRODUCTION**

Weak values have been originally defined as the average values for the results of weak measurements postselected on particular outcomes of a final strong (projective) measurement [1], where weak measurements are defined as measurements that minimally disturb the system [2]. Later on, the concept of weak values has been generalized to any POVM (positive-operator-valued measurement) and any choice of the observable and the conditioning [3]. When the outcome used for the postselection is unlikely, weak values can exceed the range of eigenvalues of the corresponding operators [4]. In correspondence of such anomalous values, the Wigner function dictating the statistical distribution of the postselected measurements takes negative values [5]. Furthermore, it can be proven that both anomalous weak values [5–7], and Wigner-function negativity [8–10], are witnesses of contextuality. Here we show that those effects occur in a paradigmatic setting of waveguide quantum electrodynamics where energy exchanges feature anomalous weak values. The setting is the so-called one-dimensional (1D) atom, a two-level emitter (qubit) interacting with an electromagnetic field propagating in 1D. When the field is prepared in a coherent state resonant with the qubit's transition this system implements a single-qubit gate with a fidelity limited by the buildup of qubit-field correlations [11]. Weak values arise in the 1D atom when the electromagnetic field is monitored via heterodyne detection

and the data are postselected over the outcomes of a qubit's projective measurement. This may be understood by regarding the propagating field as a weak measurement apparatus for the qubit [12,13], see Fig. 1(a). Superconducting circuits represent the ideal setup to implement such a detection scheme, as they grant independent access to the states of qubit and field. A recent experiment on a superconducting single-qubit gate [22] showed anomalous weak values of the field's energy change, i.e., values exceeding by far the single quantum of energy that qubit and field can physically exchange, see Fig. 1(b).

We study the 1D atom using a collision model [14], where individual temporal modes of the electromagnetic field locally interact with the qubit in a sequential fashion [15,16]. When the field is prepared in a resonant coherent state, this method provides the exact analytical expression of the qubit-field entangled state at any time [17]. From the collision model of the driven 1D atom, we derive the analytical expression of the field's Husimi-Q function conditioned on the outcomes of the final qubit's measurement. This function gives access to all the moments of the postselected heterodyne distribution, namely, the field's weak values. Then we use the conditional Husimi-Q function to derive the weak value of the field's energy change, and we show that in the typical working regime of single-qubit gates, it takes anomalous values as observed in [22]. Finally, we explore the relation between anomalous weak values and negativity of the corresponding Wigner function. By exploiting the analytical expression of the field's state

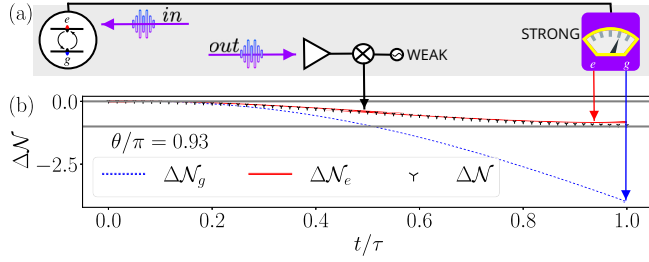


FIG. 1. Detection of the field's weak values in the single-qubit gate. (a) Schematics of the detection. The gate is implemented by coherently driving a 1D atom with a pulse of area $\theta = \Omega\tau$. The output field is continuously detected in the time interval $[0, \tau]$ with a heterodyne measurement (weak measurement), and at time τ a projective (strong) measurement is performed on the qubit and the heterodyne data acquired are postselected according on the outcome. (b) Change of the number of field excitations as a function of time. The plot shows the weak values $\Delta\mathcal{N}_e$ (solid red line) and $\Delta\mathcal{N}_g$ (dotted blue line) corresponding to postselection over the qubit's excited and ground states, respectively, and the unconditional value $\Delta\mathcal{N}$ (black chicken foot). The values of $\Delta\mathcal{N}_g$ below the solid gray line (-1) are dubbed anomalous. The plot has been obtained for a driving pulse of area $\theta = 0.93\pi$ and duration $\tau = 3/40\gamma^{-1}$, with γ being the emitter's decaying rate. This choice of parameters makes well visible the emergence of anomalous weak values and is otherwise arbitrary.

obtained with the collision model, we compute the field's conditional Wigner function and we show that anomalous weak values and Wigner-function negativities arise for the same values of the gate's angle.

The paper is organized as follows: In Sec. II we describe the coherently driven 1D atom and present the collision model of its dynamics. In Sec. III we present our main results—the analytical derivations of the field's conditional Husimi-Q function and the weak value of the field's energy change. In Sec. IV we derive the conditional Wigner function. Finally, in Sec. V we draw the conclusions of our work.

II. SYSTEM AND MODEL

A. The coherently driven 1D atom

The 1D atom comprises a qubit coupled to a single-mode, semi-infinite waveguide. The waveguide field constitutes a reservoir of electromagnetic modes of frequencies ω_k and linear momentum $k = \omega_k v^{-1}$, with v being the field's group velocity taken as positive. These modes are destroyed (created) by the operators $a_k(a_k^\dagger)$. The dynamics of the joint system is ruled by the Hamiltonian

$$H = \left[\hbar\omega_0\sigma^\dagger\sigma + \hbar\sum_{k=0}^{\infty}\omega_k a_k^\dagger a_k \right] + i\hbar g \sum_{k=0}^{\infty} (\sigma^\dagger a_k - a_k^\dagger \sigma), \quad (1)$$

where $\sigma \equiv |g\rangle\langle e|$, with $|g(e)\rangle$ being the ground (excited) state of the emitter. Writing the above Hamiltonian, we implicitly

assumed that the light-matter interaction is weak enough that only frequency modes close to the qubit's frequency ω_0 play a role (quasimonochromatic approximation) [16]. In this regime, the rotating-wave approximation is allowed [18], and the coupling g can be considered uniform in frequency [19].

The field's lowering operator at the position x in the interaction picture [15–17] is given by

$$b(x, t) = \sqrt{\frac{1}{\varrho}} \sum_k e^{-i\omega_k(t-x/v)} a_k = b(0, t - x/v), \quad (2)$$

where ϱ is the modes' density verifying the relation $\sum_k e^{-i\omega_k(t-t')}/\varrho = \delta(t-t')$. The operators $b(0, t)$ satisfy the bosonic commutation relation, i.e., $[b(0, t), b^\dagger(0, t')] = \delta(t-t')$ [16]. The qubit is located at the position $x = 0$ of the waveguide, such that the interaction picture Hamiltonian reads

$$H_I(t) = i\hbar\sqrt{\gamma}(\sigma^\dagger(t)b(0, t) - b^\dagger(0, t)\sigma(t)), \quad (3)$$

where we defined the interaction picture lowering operator $\sigma(t) = e^{-i\omega_0 t}\sigma$, and the emitter's decay rate $\gamma = g^2\varrho$. In the regions where $x < 0$ or $x > 0$, the field travels without deformation. It is then natural to define field's input and output operators, respectively, as $b_{\text{in}}(t) \equiv \lim_{\epsilon \rightarrow 0^-} b(\epsilon, t)$, and $b_{\text{out}}(t) \equiv \lim_{\epsilon \rightarrow 0^+} b(\epsilon, t)$. These operators satisfy the mean input-output relation $\langle b_{\text{out}}(t) \rangle = \langle b_{\text{in}}(t) \rangle - \sqrt{\gamma}\langle \sigma(t) \rangle$, in agreement with the textbook input-output relation written in the Heisenberg representation [19].

The gate's input field is a square coherent pulse of amplitude $\langle b_{\text{in}}(t) \rangle = \alpha_t = \alpha e^{-i\omega_0 t}/\sqrt{\varrho}$, with α real. Hence the field's state at the initial time ($t = 0^-$) reads $|\alpha\rangle \equiv \mathcal{D}(\alpha)|0\rangle$, where $\mathcal{D}(\alpha) = e^{(\alpha a_0^\dagger - \alpha^* a_0)}$ is the displacement operator of the mode with frequency ω_0 , which can be equivalently written as $\mathcal{D}(\alpha) = e^{\int dt (\alpha b^\dagger(t) - \alpha^* b(t))}$ using the transformation (2). A unitary driving on the qubit, $H_D(t)$, arises naturally when displacing the interaction Hamiltonian in Eq. (3), $\mathcal{D}(-\alpha)H_I(t)\mathcal{D}(\alpha) = H_I(t) - \Omega\sigma_y/2 = H_I(t) + H_D(t)$, with $\Omega/2 = g\alpha$ and $\sigma_y = i\sigma^\dagger - i\sigma$. In the classical limit of the field [11], the qubit-reduced dynamics is solely dictated by $H_D(t)$ and hence it reduces to a pure rotation around the y axis of an angle $\theta = \Omega\tau$, where τ is the duration of the qubit-field interaction. In this limit, the light-matter interaction (int) is equivalent to the map:

$$|g\rangle \otimes |\alpha\rangle \xrightarrow{\text{int}(\tau)} [\cos(\theta/2)|g\rangle + \sin(\theta/2)|e\rangle] \otimes |\alpha\rangle.$$

Beyond the classical limit, the interaction entangles qubit and field, resulting in a loss of purity of the reduced qubit's state and a degradation of the coherence of the input field. The joint qubit-field state at time τ can be written as the pure state:

$$|\Psi(\tau)\rangle = \sqrt{P_g(\tau)}|g\rangle, \psi_g(\tau) + \sqrt{P_e(\tau)}|e\rangle, \psi_e(\tau)$$

with

$$|\psi_\epsilon(\tau)\rangle = \mathcal{D}(\alpha) \left(\frac{f_\epsilon^{(0)}(\tau) - \int_0^\tau dt f_\epsilon^{(1)}(\tau, t) e^{-i\omega_0 t} b^\dagger(t) + \dots}{\sqrt{P_\epsilon(\tau)}} \right) |0\rangle, \quad (4)$$

where $\epsilon = g, e$, and we adopted the short notation $b(t) \equiv b(0, t)$. The state in the parenthesis is the field state in the displaced reference frame, where the interaction Hamiltonian is $\mathcal{D}(-\alpha)H_I(t)\mathcal{D}(\alpha)$, and the input field is the vacuum. In such a frame, the only mechanism responsible for the photons' creation is the spontaneous emission, and hence the field coincides with the emitter's fluorescence having amplitude $\langle b_{\text{out}}(t) \rangle - \langle b_{\text{in}}(t) \rangle = -\sqrt{\gamma}\langle\sigma(t)\rangle$. The ellipsis represents the components with $j > 1$ spontaneously emitted photons, having the form $(-)^j \int dt_j f_\epsilon^{(j)}(\tau, \mathbf{t}_j) e^{-i\omega_0 t_1} b^\dagger(t_1) \dots e^{-i\omega_0 t_j} b^\dagger(t_j) |0\rangle$, with $\mathbf{t}_j = \{t_1, t_2, \dots, t_j\}$. The functions $f_\epsilon^{(j)}(\tau, \mathbf{t}_j)$ are real, and their explicit expression has been derived in [17] and reported in the Appendix A. Since their amplitude is proportional to $\gamma^{j/2}$, the components with $j > 2$ can be neglected in the regime usually considered in single-qubit gates where $\Omega \gg \gamma$. We can define the probability that the qubit spontaneously emits j photons during the evolution from $|g\rangle$ to $|\epsilon\rangle$ as $p_\epsilon^{(j)}(\tau) \equiv \int dt_j |f_\epsilon^{(j)}(\tau, \mathbf{t}_j)|^2 / P_\epsilon(\tau)$.

B. Collision model of the coherently driven 1D atom

We now define adimensional discrete-temporal modes of the electromagnetic field [15–17], i.e., $b_n \equiv \sqrt{\Delta t} b(t_n)$, where Δt is an infinitesimal time increment, n is an integer number, and $[b_n, b_{n'}^\dagger] = \delta_{n,n'}$, with $\delta_{n,n'}$ being the Kronecker delta [15,16]. The initial state of the field can be written in terms of the discrete-temporal modes as $|\alpha\rangle = \bigotimes_n |\alpha_n\rangle$, where $|\alpha_n\rangle = \mathcal{D}^{(n)}(\alpha_n) |0_n\rangle$, with $\mathcal{D}^{(n)}(\alpha_n) = e^{(\alpha_n b_n^\dagger - \alpha_n^* b_n)}$ and $\alpha_n = \sqrt{\Delta t} / \rho \alpha e^{-i\omega_0 t_n}$.

We can write the infinitesimal unitary evolution operator $U(t_{n+1} - t_n)$ as

$$U^{(n)} \equiv U(t_{n+1} - t_n) \approx \exp \left\{ -\frac{i}{\hbar} \Delta t H_I(t_n) \right\}, \text{ with}$$

$$H_I(t_n) \equiv i\hbar \sqrt{\frac{\gamma}{\Delta t}} (\sigma^\dagger(t_n) b_n - b_n^\dagger \sigma(t_n)). \quad (5)$$

The joint system evolution can be decomposed in a sequence of collisions:

$$\rho(t_{n+1}) = U^{(n)} \rho(t_n) U^{(n)\dagger}. \quad (6)$$

The qubit's reduced state at time t_{n+1} can be found by tracing Eq. (6) over the state of the n th temporal mode prepared in the state $|\alpha_n\rangle$:

$$\rho_q(t_{n+1}) = \text{Tr}_n \{ U^{(n)} \rho_q(t_n) |\alpha_n\rangle \langle \alpha_n| U^{(n)\dagger} \}. \quad (7)$$

As expected, expanding $U^{(n)}$ at the second order in Δt , Eq. (7) becomes a discrete-time Lindblad master equation [15,16]:

$$\frac{\rho_q(t_n) - \rho_q(t_{n-1})}{\Delta t} = \frac{\Omega}{2} [\sigma - \sigma^\dagger, \rho_q(t_{n-1})] + \gamma \left(\sigma \rho_q(t_{n-1}) \sigma^\dagger - \frac{1}{2} \{ \sigma^\dagger \sigma, \rho_q(t_{n-1}) \} \right). \quad (8)$$

Notice that at time t_n , the $(n-1)$ -th discrete-temporal mode of the field has just interacted with the qubit, while the n th is going to interact next. Then, input and output operators

correspond to the limits:

$$b_{\text{in}}(t_n) = \lim_{\Delta t \rightarrow 0} \frac{b_n}{\sqrt{\Delta t}},$$

$$b_{\text{out}}(t_n) = \lim_{\Delta t \rightarrow 0} \frac{b_{n-1}}{\sqrt{\Delta t}}. \quad (9)$$

III. WEAK FIELD VALUES

The weak value of an operator at time t can be written as [3,13,20]

$$\langle O(t) \rangle_{f,i} = \frac{\text{Tr} \{ \Pi_f U(\tau - t) O(t) \rho_i(t) U^\dagger(\tau - t) \}}{P_f(\tau)}, \quad (10)$$

where $\Pi_f = |f\rangle \langle f|$ is the projector on the final measurement's outcome, $U(\tau - t) = \exp\{(-i/\hbar) \int_t^\tau dt' H_I(t')\}$, and $\rho_i(t) = U(t) |i\rangle \langle i| U^\dagger(t)$ is the system's state at time t starting from the pure state $|i\rangle$. From now on we will consider that the joint qubit-field system starts its evolution from the state $|g, \alpha\rangle$, and that the qubit is measured in its energy basis at the final time τ . Then, in the rest of the paper, we will simplify the weak values' notation by omitting the subscript that refers to the initial state and by using $\epsilon = e, g$ to denote the possible outcomes of the qubit's final measurement.

We are particularly interested in the weak values of the output field's quadratures, $\text{Re}\{\langle b_{\text{out}}(t) \rangle_\epsilon\}$ and $\text{Im}\{\langle b_{\text{out}}(t) \rangle_\epsilon\}$, and intensity, $\langle b_{\text{out}}^\dagger(t) b_{\text{out}}(t) \rangle_\epsilon$. Indeed, these quantities can be measured by implementing the driven 1D atom with a superconducting circuit, performing heterodyne detection on the output field, and postselecting it on the outcomes of the final qubit's measurement as in Refs. [21,22].

Furthermore, from the weak value of the output intensity, we can derive the weak value of the change of the field's number of excitations:

$$\Delta N_\epsilon \equiv \int_0^\tau dt \langle b_{\text{out}}^\dagger(t) b_{\text{out}}(t) \rangle_\epsilon - |\alpha_t|^2 \tau. \quad (11)$$

In the typical regime used to perform single-qubit gates, i.e., $\Omega \gg \gamma$, this quantity may take anomalous values, namely, values exceeding by far the single quantum of excitation that the field can physically exchange with the qubit, i.e., $|\Delta N_\epsilon| > 1$, see Fig. 1(b), and Refs. [22,23].

Using the collision model picture introduced in the previous section, we can derive explicit expressions of the weak values of any field's operator of the kind $O(t) = (b_{\text{out}}^\dagger(t))^m (b_{\text{out}}(t))^l$, hence including output quadratures and intensity. The first step is to write these weak values in terms of the discrete-time output operator [Eq. (9)]:

$$\begin{aligned} & \langle (b_{\text{out}}^\dagger(t_n))^m (b_{\text{out}}(t_n))^l \rangle_\epsilon \\ &= \lim_{\Delta t \rightarrow 0} \frac{\text{Tr} \{ \Pi_\epsilon U(\tau - t_n) (b_{n-1}^\dagger)^m b_{n-1}^l \rho(t_n) U^\dagger(\tau - t_n) \}}{\sqrt{\Delta t}} \\ &= \lim_{\Delta t \rightarrow 0} \frac{\langle \psi_\epsilon(\tau) | (b_{n-1}^\dagger)^m b_{n-1}^l | \psi_\epsilon(\tau) \rangle}{\sqrt{\Delta t}}, \end{aligned} \quad (12)$$

where we used the fact that b_{n-1} commutes with $U(\tau - t_n)$. Equation (12) shows that the weak value of an arbitrary observable of the output field is simply its average value on the state $|\psi_\epsilon(t)\rangle$ given in Eq. (4).

Hence, to evaluate Eq. (12) we can use the conditional Husimi-Q function of the n th temporal mode:

$$Q_\epsilon^{(n)}(s) \equiv \frac{1}{\pi} \text{Tr}\{\Pi_s^{(n)} |\psi_\epsilon(\tau)\rangle \langle \psi_\epsilon(\tau)|\}, \quad (13)$$

where $\Pi_s^{(n)} = |s_n\rangle \langle s_n|$, with $|s_n\rangle = \mathcal{D}^{(n)}(s) |0_n\rangle$ and $\mathcal{D}^{(n)}(s) = e^{(sb_n^\dagger - s^*b_n)}$ being the displacement operator of the n th temporal mode. From the Husimi function it is possible to obtain any moment of the output field's distribution just performing an integral in the complex plane [24]. So, for instance, the weak value of the output intensity at time t_n can be obtained from

$$\begin{aligned} Q_\epsilon^{(n)}(s) &= \frac{1}{\pi P_\epsilon(\tau)} \text{Tr}\{E_\epsilon(\tau, t_{n+1}) \langle s_n | U^{(n)} | \alpha_n \rangle \rho_q(t_n) \langle \alpha_n | (U^{(n)})^\dagger | s_n \rangle\} \\ &= \text{Tr}\{E_\epsilon(\tau, t_{n+1}) [\rho_q(t_{n+1}) + \gamma \Delta t (|\alpha_n - s|^2 - 1) \sigma \rho_q(t_n) \sigma^\dagger + \sqrt{\gamma \Delta t} ((\alpha_n - s)^* \sigma(t_n) \rho_q(t_n) + (s - \alpha_n) \rho_q(t_n) \sigma^\dagger(t_n))] \} \\ &\quad \times \frac{\exp\{-|s - \alpha_n|^2\}}{\pi P_\epsilon(\tau)}. \end{aligned} \quad (16)$$

Noticing that $\text{Tr}\{E_\epsilon(\tau, t_{n+1}) \sigma(t_n) \rho_q(t_n)\} / P_\epsilon(\tau) = \langle \sigma(t_n) \rangle_\epsilon$ [25], and that $\text{Tr}\{E_\epsilon(\tau, t_{n+1}) \rho_q(t_{n+1})\} = P_\epsilon(\tau)$, we find

$$\begin{aligned} Q_\epsilon^{(n)}(s) &= \frac{e^{-|s - \alpha_n|^2}}{\pi} [1 + (|\alpha_n - s|^2 - 1) \gamma \Delta t \mathcal{J}_\epsilon(t_n) \\ &\quad + 2\sqrt{\gamma \Delta t} \text{Re}\{(s - \alpha_n) \langle \sigma(t_n) \rangle_\epsilon\}], \end{aligned} \quad (17)$$

where we defined

$$\gamma \mathcal{J}_\epsilon(t_n) = \text{Tr}\{\Pi_\epsilon U(\tau - t_n) \sigma \rho_q(t_n) \sigma^\dagger U^\dagger(\tau - t_n)\} / P_\epsilon(\tau).$$

An alternative, although equivalent, derivation of the conditional Husimi-Q function from the wave function in Eq. (4) is reported in the Appendix B.

Using Eq. (17) to perform the integral in Eq. (14) and then plugging the result in Eq. (11), we find

$$\Delta \mathcal{N}_\epsilon = \int_0^\tau dt [\gamma \mathcal{J}_\epsilon(t) - \Omega \text{Re}\{\langle \sigma(t) \rangle_\epsilon\}]. \quad (18)$$

Notice that $\int_0^\tau dt \gamma \mathcal{J}_\epsilon(t) = \sum_{j \geq 1} p_\epsilon^{(j)}(\tau) / P_\epsilon(\tau)$ is the total probability that the qubit undergoes spontaneous emission along its evolution from $|g\rangle$ to $|\epsilon\rangle$. While the last term, $-\int_0^\tau dt \Omega \text{Re}\{\langle \sigma(t) \rangle_\epsilon\} = 2 \int_0^\tau dt \text{Re}\{\langle b_{\text{in}}(t) \rangle^* \langle b_{\text{out}}(t) \rangle_\epsilon - \langle b_{\text{in}}(t) \rangle\}$, features an interference between the input field and the emitter's fluorescence postselected over the outcome ϵ , this term is the only part of $\Delta \mathcal{N}_\epsilon$ whose modulus can exceed 1, leading to anomalous values.

IV. CONDITIONAL WIGNER FUNCTION

In the previous section we derived the conditional Husimi-Q function of the field's temporal modes to predict the results of a continuous heterodyne detection with postselection. Here instead we consider the mode of frequency ω_0 being the qubit's frequency and the center of the field's spectrum. In the quasimonochromatic, the resonant regime usually employed in single-qubit gates ω_0 is much more

$Q_\epsilon^{(n)}(s)$ by doing the integral:

$$\langle b_{\text{out}}^\dagger(t_n) b_{\text{out}}(t_n) \rangle_\epsilon = \lim_{\Delta t \rightarrow 0} \frac{1}{\Delta t} \int d^2s (|s|^2 - 1) Q_\epsilon^{(n)}(s). \quad (14)$$

The explicit expression of $Q_\epsilon^{(n)}(s)$ in terms of qubit's operators can be computed using the collision model. This is the main result of this section. First, we rewrite Eq. (13) as

$$Q_\epsilon^{(n)}(s) = \frac{1}{\pi P_\epsilon(\tau)} \text{Tr}\{E_\epsilon(\tau, t_{n+1}) \Pi_s^{(n)} \rho(t_{n+1}) \Pi_s^{(n)}\}, \quad (15)$$

where $E_\epsilon(\tau, t) \equiv U^\dagger(\tau - t) |\epsilon\rangle \langle \epsilon| U(\tau - t)$ is the so-called effect matrix [25]. Now, plugging Eq. (7) in Eq. (15), and expanding $U^{(n)}$ at the second order in Δt , we find

populated than the other frequencies, so $\mathcal{N}(\omega_0) \equiv \langle a_0^\dagger a_0 \rangle \approx \int_0^\tau dt \langle b^\dagger(t) b(t) \rangle$, and consequently, $\Delta \mathcal{N}_\epsilon(\omega_0) \equiv \langle a_0^\dagger a_0 \rangle_\epsilon - |\alpha|^2 \approx \Delta \mathcal{N}_\epsilon$, with $\Delta \mathcal{N}_\epsilon$ given by Eq. (18) (see the Appendix C).

The expectation value of the number operator $a_0^\dagger a_0$ can be equivalently found using either its Glauber-Sudarshan, Husimi, or Wigner quasiprobability distributions [24]. The latter is particularly interesting, as its negative values certify the quantum nature of the electromagnetic field [26] and may witness contextuality [8–10], exactly as anomalous weak values [5–7]. For this reason here we derive the conditional Wigner function of the mode of frequency ω_0 :

$$\begin{aligned} \mathcal{W}_\epsilon(\mu) &\equiv \frac{1}{\pi^2} \int d^2\lambda e^{-\lambda \mu^* + \lambda^* \mu} \text{Tr}\{e^{-\lambda^* a_0 + \lambda a_0^\dagger} |\psi_\epsilon(\tau)\rangle \langle \psi_\epsilon(\tau)|\} \\ &= \frac{2e^{-2|\mu - \alpha|^2}}{\pi P_\epsilon(\tau)} [(P_\epsilon(\tau) - |\tilde{f}_\epsilon^{(1)}(\tau, 0)|^2) \\ &\quad - |\tilde{f}_\epsilon^{(1)}(\tau, 0)|^2 (1 - 4|\mu - \alpha|^2) \\ &\quad - 4\text{Re}\{\tilde{f}_\epsilon^{(1)*}(\tau, 0) f_\epsilon^{(0)}(\tau) (\mu - \alpha)\} + \dots], \end{aligned} \quad (19)$$

where $\tilde{f}_\epsilon^{(1)}(\tau, \omega_k - \omega_0) = \sqrt{\frac{1}{\Omega}} \int_0^\tau dt f_\epsilon^{(1)}(\tau, t) e^{-i(\omega_k - \omega_0)t}$, and $|\tilde{f}_\epsilon^{(1)}(\tau, 0)|^2 / P_\epsilon(\tau)$ is the probability that the qubit spontaneously emits one photon of frequency ω_0 . In the limit of monochromatic emission, no photon with frequency $\omega_k \neq \omega_0$ is emitted, hence $|\tilde{f}_\epsilon^{(1)}(\tau, 0)|^2 = p^{(1)}(\tau)$. The explicit derivation of Eq. (19), including the terms coming from the multiphoton emission (ellipses), is given in Appendix C.

Figure 2 shows the main result of this section: the conditional Wigner function $\mathcal{W}_\epsilon(\mu)$ takes negative values when $\Delta \mathcal{N}_\epsilon$ takes anomalous values. Figure 2(a) shows the values of $\Delta \mathcal{N}_\epsilon$ varying the gate's angle θ in $[0, \pi]$. While $\Delta \mathcal{N}_\epsilon$ remains between 0 and -1 , $\Delta \mathcal{N}_g$ takes anomalous values (smaller

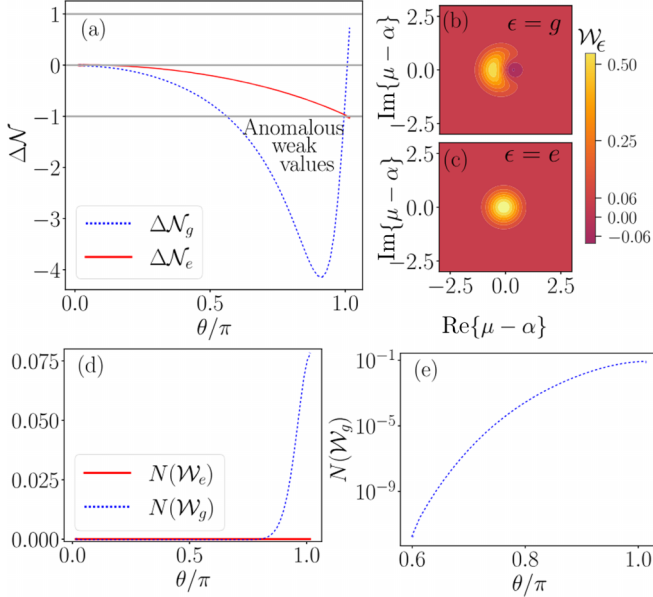


FIG. 2. Anatomy of the single-qubit gate. (a) Weak values of the change of the number of field excitations as a function of the gate angle, $\Delta\mathcal{N}_e$ (solid red line) and $\Delta\mathcal{N}_g$ (dotted blue line). (b, c) Color plots of the conditional Wigner functions \mathcal{W}_g and \mathcal{W}_e for $\theta/\pi = 0.93$. (d) Wigner-function negativity, $N(\mathcal{W}_e) = \int d^2\mu |\mathcal{W}_e(\mu)| - 1$, as a function of θ : \mathcal{W}_e (solid red line) is always positive, while \mathcal{W}_g (dotted blue line) can take negative values in the region of anomalous weak values of $\Delta\mathcal{N}_g$. (e) Plot of \mathcal{W}_g (log scale) in the region of anomalous values of $\Delta\mathcal{N}_g$, i.e., $\theta \in [0.6\pi, \pi]$. All the plots have been obtained for $\tau = 3/40\gamma^{-1}$. The choice of parameters makes well visible the emergence of anomalous weak values and the Wigner-function negativity and is otherwise arbitrary.

than -1) for some gate's angle. Figures 2(d)–2(e) show the Wigner function's negativity, $N(\mathcal{W}_e) \equiv \int d^2\mu |\mathcal{W}_e(\mu)| - 1$ [26]. This quantity is zero when $\mathcal{W}_e(\mu)$ is non-negative for every μ and bigger than zero otherwise. The plot shows $N(\mathcal{W}_e)$ is zero for every value of θ in the range $[0, \pi]$, see Fig. 2(d), while $N(\mathcal{W}_g)$ is nonzero for all the values of θ such that $\Delta\mathcal{N}_g$ is smaller than -1 , see Fig. 2(e).

V. CONCLUSION

We presented an anatomical study of a single-qubit gate implemented with a 1D atom driven by a coherent field at resonance. The scattered field is continuously monitored via heterodyne and postselected over the outcomes of a qubit's projective measurement. Using a collision model, we derived the analytical expression of the field's Husimi-Q function conditioned on the outcomes of the qubit's measurement. The conditional Husimi grants access to all the

moments of the postselected heterodyne distribution, i.e., the field's weak values. In particular, we used the conditional Husimi-Q function to derive the weak value of the field's energy change. As recently observed in [22], this quantity can exceed by far the single quantum, hence reaching anomalous values. Using the analytical expression of the atom-field wave function, we derived the field's conditional Wigner functions. Then we showed that, as expected from general foundational results [5], anomalous weak values of the energy change correspond to nonzero Wigner-function negativity.

ACKNOWLEDGMENTS

We warmly thank Mattia Walschaers for his helpful advice. We gratefully acknowledge financial support from the European Union's Horizon 2020 Research and Innovation Program under the Marie Skłodowska-Curie Grant Agreement No. 861097, the Foundational Questions Institute Fund (Grants No. FQXi-IAF19-01 and No. FQXi-IAF19-05), the John Templeton Foundation (Grant No. 61835), and the ANR Research Collaborative Project “Qu-DICE” (Grant No. ANR-PRCCES47).

APPENDIX A: EXPLICIT EXPRESSION OF THE FIELD'S WAVE FUNCTION

Explicit expressions of the functions $f_e^{(j)}(\tau, \mathbf{t}_j)$, for the joint system's initial state being $|g, \alpha\rangle$, have been derived in [17]. Here we report them for the sake of completeness:

$$f_g^{(0)}(t) = e^{-\gamma t/4} [\cos(\Omega' t/2) + \sin(\Omega' t/2)(\gamma)/(2\Omega')], \quad (\text{A1})$$

$$f_e^{(0)}(t) = e^{-\gamma t/4} \sin(\Omega' t/2)\Omega/\Omega'. \quad (\text{A2})$$

The amplitudes of the emitted photons read

$$f_e^{(1)}(\tau, t) = \sqrt{\gamma} f_e^{(0)}(\tau - t) e^{-i\omega_0 t} f_e^{(0)}(t), \quad (\text{A3})$$

$$f_e^{(j>1)}(\tau, \mathbf{t}_j) = (\sqrt{\gamma})^j f_e^{(0)}(\tau - t_j) e^{-i\omega_0 t_j} \times \left[\prod_{i=2}^j f_e^{(0)}(t_i - t_{i-1}) e^{-i\omega_0 t_{i-1}} \right] f_e^{(0)}(t_1), \quad (\text{A4})$$

where $\Omega' = \sqrt{(\Omega)^2 - \gamma^2/4}$.

APPENDIX B: ALTERNATIVE DERIVATION OF THE HUSIMI FUNCTION

The field's wave function in Eq. (4) can be rewritten in terms of discrete-temporal modes:

$$|\psi_e(\tau)\rangle = \frac{\bigotimes_n \mathcal{D}^{(n)}(\alpha_n) (f_e^{(0)}(\tau) - \sum_{n=0}^{N-1} \sqrt{\Delta t} f_e^{(1)}(\tau, t_n) e^{-i\omega_0 t_n} b_n^\dagger) + \dots}{\sqrt{P_e(\tau)}} |0\rangle, \quad (\text{B1})$$

where $N = \tau/\Delta t$.

The conditional Husimi function can be equivalently computed from the wave function (B1), including also the

components arising from the spontaneous emission of two photons. The components with $j > 2$ are irrelevant in the

present study, as they can be neglected in the typical gate regime ($\gamma \ll \Omega$), but they can be included following a conceptually analogous derivation. $\mathcal{Q}_\epsilon^{(n)}(s)$ can be rewritten as

$$\mathcal{Q}_\epsilon^{(n)}(s) \equiv \frac{1}{\pi} \text{Tr} \{ \Pi_{s-\alpha_n}^{(n)} \eta_\epsilon^{(n)} \}, \quad (\text{B2})$$

where $\eta_\epsilon^{(n)}$ is the reduced density matrix of mode b_n , written in the displaced reference frame, and $\Pi_{s-\alpha_n}$ projects it over the coherent state of amplitude $s - \alpha_n$. The field state in the displaced reference frame (now including the components with two photons emitted) reads

$$\begin{aligned} |\phi_\epsilon\rangle = & \frac{1}{\sqrt{P_\epsilon(\tau)}} \left(f_\epsilon^{(0)}(\tau) - \sum_n \sqrt{\Delta t} f_\epsilon^{(1)}(\tau, t_n) e^{-i\omega_0 t_n} b_n^\dagger \right. \\ & \left. + \sum_n \sum_{m>n} \Delta t f_\epsilon^{(2)}(\tau, t_n, t_m) e^{-i\omega_0(t_n+t_m)} b_n^\dagger b_m^\dagger \right) |0\rangle. \end{aligned} \quad (\text{B3})$$

Taking the trace over all the discrete-time modes $m \neq n$, we find $\eta_\epsilon^{(n)}$:

$$\begin{aligned} \eta_\epsilon^{(n)} = & \text{Tr}_{\otimes m \neq n} |\phi_\epsilon\rangle \langle \phi_\epsilon| \\ = & \frac{1}{P_\epsilon(\tau)} \left[|\phi_\epsilon^{01}\rangle \langle \phi_\epsilon^{01}| + \sum_{m \neq n} |\phi_\epsilon^{12}(m)\rangle \langle \phi_\epsilon^{12}(m)| \right. \\ & \left. + \Delta t^2 \sum_{m \neq n} \sum_{l \neq n} |f_\epsilon^{(2)}(\tau, t_m, t_l)|^2 |0_n\rangle \langle 0_n| \right], \end{aligned} \quad (\text{B4})$$

where

$$|\phi_\epsilon^{01}\rangle = f_\epsilon^{(0)}(\tau) |0_n\rangle - \sqrt{\Delta t} f_\epsilon^{(1)}(\tau, t_n) e^{-i\omega_0 t_n} |1_n\rangle, \quad (\text{B5})$$

and

$$\begin{aligned} |\phi_\epsilon^{12}(m)\rangle = & -\sqrt{\Delta t} f_\epsilon^{(1)}(\tau, t_m) e^{-i\omega_0 t_m} |0_n\rangle + \Delta t (f_\epsilon^{(2)}(\tau, t_n, t_m) \\ & + f_\epsilon^{(2)}(\tau, t_m, t_n)) e^{-i\omega_0(t_n+t_m)} |1_n\rangle. \end{aligned} \quad (\text{B6})$$

Plugging Eq. (B4) into Eq. (B2), we obtain

$$\begin{aligned} \mathcal{Q}_\epsilon^{(n)}(s) = & \frac{e^{-|s-\alpha_n|^2}}{\pi P_\epsilon(\tau)} \left[P_\epsilon(\tau) + \Delta t \left(|f_\epsilon^{(1)}(\tau, t_n)|^2 \right. \right. \\ & + \sum_{m>n} \Delta t |f_\epsilon^{(2)}(\tau, t_n, t_m)|^2 \\ & + \sum_{m<n} \Delta t |f_\epsilon^{(2)}(\tau, t_m, t_n)|^2 \left. \right) (|\alpha_n - s|^2 - 1) \\ & - 2\sqrt{\Delta t} \text{Re} \left\{ e^{i\omega_0 t_n} (s - \alpha_n) (f_\epsilon^{(1)}(\tau, t_n) f_\epsilon^{(0)}(\tau) \right. \\ & + \sum_{m>n} \Delta t f_\epsilon^{(2)}(\tau, t_n, t_m) f_\epsilon^{(1)}(\tau, t_m) \\ & \left. \left. + \sum_{m<n} \Delta t f_\epsilon^{(2)}(\tau, t_m, t_n) f_\epsilon^{(1)}(\tau, t_m) \right) \right] \}. \end{aligned} \quad (\text{B7})$$

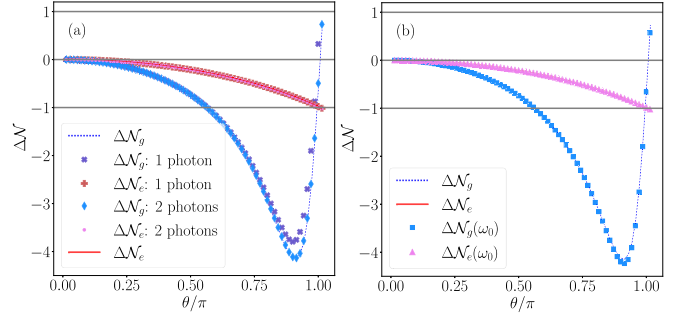


FIG. 3. (a) Comparison between $\Delta \mathcal{N}_\epsilon$ as a function of θ computed using different truncations of the field's wave function. The gate considered has $\gamma\tau = 3/40$. The exact values of $\Delta \mathcal{N}_\epsilon$ (solid red line) and $\Delta \mathcal{N}_g$ (dotted blue line) have been computed from Eq. (18) by numerical integration of the qubit's forward and backwards Lindblad master equation, see Ref. [25]. The weak values computed truncating the field's wave function at the component with two photons emitted, see Eq. (B8); $\Delta \mathcal{N}_\epsilon$ (pink circle) and $\Delta \mathcal{N}_g$ (light blue diamond) match the exact solutions. The weak values computed with the truncation at 1 photon emitted, $\Delta \mathcal{N}_\epsilon$ (brown plus) and $\Delta \mathcal{N}_g$ (purple cross), diverge from the exact result after $\theta \approx 0.8\pi$. (b) Comparison between the exact change in the total field's number of excitations $\Delta \mathcal{N}_\epsilon$ and the change of the field's number of excitations with frequency ω_0 , $\Delta \mathcal{N}_\epsilon(\omega_0)$ (pink triangle), $\Delta \mathcal{N}_g(\omega_0)$ (light blue square) in the considered regime. The mismatch among the two data sets is negligible, i.e., the output field can be considered as monochromatic.

Using this expression we find the following average change in the photon number:

$$\begin{aligned} \Delta \mathcal{N}_\epsilon = & \frac{1}{P_\epsilon(\tau)} \left(p_\epsilon^{(1)}(\tau) + p_\epsilon^{(2)}(\tau) \right. \\ & - 2\text{Re} \left\{ f_\epsilon^{(0)}(\tau) \int_0^\tau dt \alpha_t^* e^{-i\omega_0 t} f_\epsilon^{(1)}(\tau, t) \right\} \\ & - 2\text{Re} \left\{ \int_0^\tau dt \int_t^\tau dt' f_\epsilon^{(1)}(\tau, t') \alpha_t^* e^{-i\omega_0 t} f_\epsilon^{(2)}(\tau, t, t') \right. \\ & \left. + \int_0^\tau dt \int_0^t dt' f_\epsilon^{(1)}(\tau, t') \alpha_t^* e^{-i\omega_0 t} f_\epsilon^{(2)}(\tau, t', t) \right\} \}. \end{aligned} \quad (\text{B8})$$

Figure 3(a) shows that, in the regime considered, i.e., $\gamma^{-1} = 8\tau$, Eq. (B8) matches the exact expression of $\Delta \mathcal{N}_\epsilon$ given in Eq. (18).

APPENDIX C: WIGNER FUNCTION OF THE MODE WITH FREQUENCY ω_0

Here we give the explicit derivation of the Wigner function in Eq. (19), including also the components arising from the spontaneous emission of two photons. The components with $j > 2$ are irrelevant in the present study, as they can be neglected in the typical gate regime ($\gamma \ll \Omega$), but they can be included following a conceptually analogous derivation. Let us first rewrite the field's wave function, Eq. (4), in terms of the frequency modes using the inverse transformation of

Eq. (2):

$$|\psi_\epsilon\rangle = \frac{\mathcal{D}(\alpha)(f_\epsilon^{(0)}(\tau) - \sum_k \tilde{f}_\epsilon^{(1)}(\tau, \omega_k - \omega_0) a_k^\dagger + \dots) |0\rangle}{\sqrt{P_\epsilon(\tau)}}, \quad (\text{C1})$$

where $\tilde{f}_\epsilon^{(1)}(\tau, \omega_k - \omega_0) = \sqrt{\frac{1}{\varrho}} \int_0^\tau dt f_\epsilon^{(1)}(\tau, t) e^{-i(\omega_k - \omega_0)t}$, and a_k destroys a photon of frequency ω_k .

Now let us notice that $\mathcal{W}_\epsilon(\mu)$ can be rewritten as

$$\mathcal{W}_\epsilon(\mu) \equiv \frac{1}{\pi^2} \int d^2\lambda e^{-\lambda(\mu - \alpha)^* + \lambda^*(\mu - \alpha)} \text{Tr}\{e^{-\lambda^* a_0 + \lambda a_0^\dagger} \zeta_\epsilon\}, \quad (\text{C2})$$

where ζ_ϵ is reduced density matrix of the mode of frequency ω_0 written in the displaced reference frame. In order to obtain ζ_ϵ let us first write the field state [Eq. (C1)] in the displaced reference frame, including the components with the two photons emitted, in terms of frequency modes:

$$|\phi_\epsilon\rangle = \frac{1}{\sqrt{P_\epsilon(\tau)}} \left(f_\epsilon^{(0)}(\tau) - \sum_k \tilde{f}_\epsilon^{(1)}(\tau, \omega_k - \omega_0) a_k^\dagger + \sum_k \sum_{k'} \tilde{f}_\epsilon^{(2)}(\tau, \omega_k - \omega_0, \omega_{k'} - \omega_0) a_k^\dagger a_{k'}^\dagger \right) |0\rangle, \quad (\text{C3})$$

where

$$\begin{aligned} \tilde{f}_\epsilon^{(2)}(\tau, \omega_k - \omega_0, \omega_{k'} - \omega_0) \\ = \frac{1}{\varrho} \int_0^\tau dt e^{-i(\omega_k - \omega_0)t} \int_0^t dt' f_\epsilon^{(2)}(\tau, t', t) e^{-i(\omega_{k'} - \omega_0)t'}. \end{aligned} \quad (\text{C4})$$

Now we can define the reduced density matrix of the mode of frequency ω_0 taking the trace over the modes with $k \neq 0$:

$$\begin{aligned} \zeta_\epsilon &= \text{Tr}_{\otimes k \neq 0} |\phi_\epsilon\rangle \langle \phi_\epsilon| \\ &= \frac{1}{P_\epsilon(\tau)} \left[|\varphi_\epsilon^{012}\rangle \langle \varphi_\epsilon^{012}| + \sum_{k \neq 0} |\varphi_\epsilon^{12}(k)\rangle \langle \varphi_\epsilon^{12}(k)| \right. \\ &\quad \left. + \sum_{k' \neq 0} \sum_{k \neq 0} |\tilde{f}_\epsilon^{(2)}(\tau, \omega_k - \omega_0, \omega_{k'} - \omega_0)|^2 |0\rangle \langle 0| \right], \end{aligned} \quad (\text{C5})$$

where

$$|\varphi_\epsilon^{012}\rangle = f_\epsilon^{(0)}(\tau) |0\rangle - \tilde{f}_\epsilon^{(1)}(\tau, 0) |1\rangle + \sqrt{2} \tilde{f}_\epsilon^{(2)}(\tau, 0, 0) |2\rangle, \quad (\text{C6})$$

and

$$|\varphi_\epsilon^{12}(k)\rangle = -\tilde{f}_\epsilon^{(1)}(\tau, \omega_k - \omega_0) |0\rangle + [\tilde{f}_\epsilon^{(2)}(\tau, 0, \omega_k - \omega_0) + \tilde{f}_\epsilon^{(2)}(\tau, \omega_k - \omega_0, 0)] |1\rangle. \quad (\text{C7})$$

The matrix ζ_ϵ can be simplified:

$$\begin{aligned} \zeta_\epsilon &= \frac{1}{P_\epsilon(\tau)} [(P_\epsilon(\tau) - |\tilde{f}_\epsilon^{(1)}(\tau, 0)|^2 - 2|\tilde{f}_\epsilon^{(2)}(\tau, 0, 0)|^2) |0\rangle \langle 0| \\ &\quad - \tilde{f}_\epsilon^{(1)*}(\tau, 0) \tilde{f}_\epsilon^{(0)}(\tau) |0\rangle \langle 1| + \text{H.c.} + |\tilde{f}_\epsilon^{(1)}(\tau, 0)|^2 |1\rangle \langle 1| \\ &\quad + \sqrt{2} \tilde{f}_\epsilon^{(2)*}(\tau, 0, 0) \tilde{f}_\epsilon^{(0)}(\tau) |0\rangle \langle 2| + \text{H.c.} \\ &\quad - \sqrt{2} \tilde{f}_\epsilon^{(2)*}(\tau, 0, 0) \tilde{f}_\epsilon^{(1)}(\tau, 0) |1\rangle \langle 2| + \text{H.c.} \\ &\quad + 2|\tilde{f}_\epsilon^{(2)}(\tau, 0, 0)|^2 |2\rangle \langle 2|], \end{aligned} \quad (\text{C8})$$

where we neglected the terms containing $\tilde{f}_\epsilon^{(2)}(\tau, 0, \omega_k - \omega_0)$ or $\tilde{f}_\epsilon^{(2)}(\tau, \omega_k - \omega_0, 0)$ with $k \neq 0$, since they correspond to the unlikely emission of two photons with frequency different from ω_0 . The Wigner function can now be computed analytically, plugging Eq. (C8) into Eq. (C2):

$$\begin{aligned} \mathcal{W}(\mu) &= \frac{2e^{-2|\mu - \alpha|^2}}{\pi P_\epsilon(\tau)} [(P_\epsilon(\tau) - |\tilde{f}_\epsilon^{(1)}(\tau, 0)|^2 \\ &\quad - 2|\tilde{f}_\epsilon^{(2)}(\tau, 0, 0)|^2) - |\tilde{f}_\epsilon^{(1)}(\tau, 0)|^2 L_1(4|\mu - \alpha|^2) \\ &\quad + 2|\tilde{f}_\epsilon^{(2)}(\tau, 0, 0)|^2 L_2(4|\mu - \alpha|^2) \\ &\quad - 8\text{Re}\{\tilde{f}_\epsilon^{(2)*}(\tau, 0, 0) \tilde{f}_\epsilon^{(1)}(\tau, 0) (\mu - \alpha)^*\} \\ &\quad \times (2|\mu - \alpha|^2 - 1) \\ &\quad + 8\text{Re}\{\tilde{f}_\epsilon^{(2)*}(\tau, 0, 0) f_\epsilon^{(0)}(\tau) (\mu - \alpha)^2\} \\ &\quad - 4\text{Re}\{f_\epsilon^{(0)}(\tau) \tilde{f}_\epsilon^{(1)*}(\tau, 0) (\mu - \alpha)\}], \end{aligned} \quad (\text{C9})$$

where $L_n(x)$ are the Laguerre polynomials. The change in the number of excitations of the field with frequency ω_0 , for the two postselections, can be computed from the corresponding Wigner functions:

$$\begin{aligned} \Delta \mathcal{N}_\epsilon(\omega_0) &= \int d^2\mu \left(|\mu|^2 - \frac{1}{2} \right) \mathcal{W}_\epsilon(\mu) - |\alpha|^2 \\ &= \frac{1}{P_\epsilon(\tau)} (|\tilde{f}_\epsilon^{(1)}(\tau, 0)|^2 \\ &\quad - 2\text{Re}\{\alpha \tilde{f}_\epsilon^{(1)*}(\tau, 0) f_\epsilon^{(0)}(\tau)\} + \dots). \end{aligned} \quad (\text{C10})$$

When the scattered field can be considered as monochromatic, $\Delta \mathcal{N}_\epsilon(\omega_0) \approx \Delta \mathcal{N}_\epsilon$ [see Fig. 3(b)].

- [1] Y. Aharonov, D. Z. Albert, and L. Vaidman, How the Result of a Measurement of a Component of the Spin of a Spin-1/2 Particle Can Turn Out To Be 100, *Phys. Rev. Lett.* **60**, 1351 (1988).
 [2] H. M. Wiseman and G. J. Milburn, *Quantum Measurement and Control* (Cambridge University Press, Cambridge, England, 2009).

- [3] J. Dressel, S. Agarwal, and A. N. Jordan, Contextual Values of Observables in Quantum Measurements, *Phys. Rev. Lett.* **104**, 240401 (2010).
 [4] Y. Aharonov and L. Vaidman, Properties of a quantum system during the time interval between two measurements, *Phys. Rev. A* **41**, 11 (1990).

- [5] M. F. Pusey, Anomalous Weak Values Are Proofs of Contextuality, *Phys. Rev. Lett.* **113**, 200401 (2014).
- [6] Y. Aharonov, A. Botero, S. Popescu, B. Reznik, and J. Tollaksen, Revisiting Hardy's paradox: Counterfactual statements, real measurements, entanglement and weak values, *Phys. Lett. A* **301**, 130 (2002).
- [7] N. S. Williams and A. N. Jordan, Weak Values and the Leggett-Garg Inequality in Solid-State Qubits, *Phys. Rev. Lett.* **100**, 026804 (2008).
- [8] R. W. Spekkens, Negativity and Contextuality are Equivalent Notions of Nonclassicality, *Phys. Rev. Lett.* **101**, 020401 (2008).
- [9] R. I. Booth, U. Chabaud, and P.-E. Emeriau, Contextuality and Wigner Negativity Are Equivalent for Continuous-Variable Quantum Measurements, *Phys. Rev. Lett.* **129**, 230401 (2022).
- [10] J. Haferkamp and J. Bermejo-Vega, Equivalence of contextuality and Wigner function negativity in continuous-variable quantum optics, [arXiv:2112.14788](https://arxiv.org/abs/2112.14788).
- [11] P. Bertet, S. Osnaghi, A. Rauschenbeutel, G. Nogues, A. Auffèves, M. Brune, J. Raimond, and S. Haroche, A complementary experiment with an interferometer at the quantum-classical boundary, *Nature (London)* **411**, 166 (2001).
- [12] H. M. Wiseman, Weak values, quantum trajectories, and the cavity-QED experiment on wave-particle correlation, *Phys. Rev. A* **65**, 032111 (2002).
- [13] J. Dressel, M. Malik, F. M. Miatto, A. N. Jordan, and R. W. Boyd, Colloquium: Understanding quantum weak values: Basics and applications, *Rev. Mod. Phys.* **86**, 307 (2014).
- [14] D. Cilluffo, A. Carollo, S. Lorenzo, J. A. Gross, G. M. Palma, and F. Ciccarello, Collisional picture of quantum optics with giant emitters, *Phys. Rev. Res.* **2**, 043070 (2020).
- [15] F. Ciccarello, Collision models in quantum optics, *Quantum Measurements and Quantum Metrology* **4**, 53 (2017).
- [16] J. A. Gross, C. M. Caves, G. J. Milburn, and J. Combes, Qubit models of weak continuous measurements: Markovian conditional and open-system dynamics, *Quantum Sci. Technol.* **3**, 024005 (2018).
- [17] M. Maffei, P. A. Camati, and A. Auffèves, Closed-system solution of the 1D atom from collision model, *Entropy* **24**, 151 (2022).
- [18] R. Loudon, *The Quantum Theory of Light* (Oxford University Press, Oxford, England, 2000).
- [19] C. W. Gardiner and M. J. Collett, Input and output in damped quantum systems: Quantum stochastic differential equations and the master equation, *Phys. Rev. A* **31**, 3761 (1985).
- [20] J. Dressel and A. N. Jordan, Weak Values are Universal in Von Neumann Measurements, *Phys. Rev. Lett.* **109**, 230402 (2012).
- [21] P. Campagne-Ibarcq, L. Bretheau, E. Flurin, A. Auffèves, F. Mallet, and B. Huard, Observing Interferences between Past and Future Quantum States in Resonance Fluorescence, *Phys. Rev. Lett.* **112**, 180402 (2014).
- [22] J. Stevens, D. Szombati, M. Maffei, C. Elouard, R. Assouly, N. Cottet, R. Dassonneville, Q. Ficheux, S. Zeppetzauer, A. Bienfait, A. N. Jordan, A. Auffèves, and B. Huard, Energetics of a Single Qubit Gate, *Phys. Rev. Lett.*, **129**, 110601 (2022).
- [23] S. Rogers and A. N. Jordan, Post-selection and quantum energetics, *Phys. Rev. A* **106**, 052214 (2022).
- [24] D. Walls and G. J. Milburn, Representations of the electromagnetic field, in *Quantum Optics* (Springer, New York, 2008), pp. 57–72.
- [25] S. Gammelmark, B. Julsgaard, and K. Mølmer, Past Quantum States of a Monitored System, *Phys. Rev. Lett.* **111**, 160401 (2013).
- [26] A. Kenfack and K. Życzkowski, Negativity of the Wigner function as an indicator of non-classicality, *J. Opt. B* **6**, 396 (2004).